Journal of Environmental Science International
25(7); 927~935; July 2016

pISSN: 1225-4517 eISSN: 2287-3503
http://dx.doi.org/10.5322/JESI.2016.25.7.927

ORIGINAL ARTICLE

Release of Oxygen from a Nano-sized Water Droplet Observed using Molecular Dynamics

Chang-Han Lee, Matthew Stanley Ambrosia*

Department of Environmental Administration, Catholic University of Pusan, Busan 46252, Korea

Abstract

Dissolved oxygen is necessary for many biological processes as well as many industrial practices. Dissolved oxygen released from water in dissolved air flotation (DAF) systems can be have many different applications. However, DAF systems are very costly to operate. To develop more efficient DAF systems, a deeper understanding of the process of oxygen being released from water is required. In this study, molecular dynamics (MD) simulations were used to simulate 100 oxygen molecules surrounded by 31002 water molecules at temperatures ranging from 0℃ to 100℃. Simulations were carried out for 10 ns, during which, in most cases, all the oxygen molecules were released from the water droplet. With MD simulations, visualization of the molecules escaping the water droplet was possible, which aided the understanding of the interactions between molecules at the nano-scale. The results showed that as the oxygen molecules moved near the edge of the water droplet that the oxygen molecules hesitated before escaping the water droplet or returned to the interior of the water droplet. This was because of the attractive forces between the water and oxygen molecules. Moreover, after most of the oxygen molecules were released from the droplet, some were found to return to the droplet's edge or even the interior of the droplet. It was also confirmed that oxygen molecules were released at a faster rate at higher temperatures.

Keywords : Molecular dynamics, Nanobubble, Nanodroplet, Oxygen, Dispersion

1. Introduction

Bubbles as well as dissolved gases in liquids have been studied for many years as their applications can be applied to various areas from food science to medical science to purification processes(Dickenson et al., 2002; Papadopoulou et al., 2014; Bahadori et al., 2013). Countless applications are being found to make our world more efficient and comfortable using dissolved gases. As far back as the early 1900s dissolved air flotation (DAF) has been used to separate mineral particles and a US patent was reported in 1905 pressurized aeration followed by pressure release(Sulman et al., 1905). DAF systems dissolve air under pressure and then release the air at atmospheric pressure in a flotation tank. The released air forms tiny bubbles which stick to various suspended solids reducing the apparent density of a particle causing them to float. This allows them to be removed be skimming the surface of the water. Applications are found in purifying industrial wastewater as well as treat municipal sewage(Hami et

Received 6 April, 2016; **Revised** 13 May, 2016;
Accepted 13 May, 2016
***Corresponding author** : Matthew Stanley Ambrosia, Department of Environmental Administration, Catholic University of Pusan, Busan 46252, Korea
Phone : +82-51-510-0634
E-mail : ambrosia@cup.ac.kr

al., 2007; Zhang et al., 2014). DAF systems also deal with fine-grained minerals, coal ash, low-grade slag, etc.

The main disadvantage of DAF systems is that compared to other processes is the high energy consumption. Generally pressures ranging from 3 to 6 atmospheres are used and this step can be very costly. The key to more extensive use of micro- and nanobubbles is being able to produce them more efficiently and conveniently with low cost methodologies (Zimmerman et al., 2011). The advantage of nanobubbles includes the fact that they are clean and environ -mentally friendly. Oxygen nanobubbles also have an extremely high mass transfer efficiency(Agarwal et al., 2011). Due to the weighty advantages of DAF systems on-going research is being conducted to predict air concentration using correlations and predictive tools(Bahadori et al., 2013).

While many studies have been conducted at the macro scale there still questions about bubbles at the nano-scale. With the development of molecular dynamics (MD) and the speed of computers we can attain insight into bubble dynamics as well as the dissolved gas in liquids. With the help of MD it has become known that many observed phenomenon at the macroscale cannot be seen at the nanoscale. The often used no-slip boundary condition at the macroscale is unrealistic in some cases and a wide range of conditions can be seen using molecular dynamics(Thompson and Trojan, 1997). Discrepancies in the Cassie and Wenzel predictions of water droplets on textured surfaces were also found between the macroscale and MD simulations(Ambrosia et al., 2013). MD simulations of Argon molecules in a nanochannel were conducted by Nagayama et al. (2006). It was observed that the temperature and pressure inside a bubble disagrees with the prediction of the macroscopic Young-Laplace equation. Connecting phenomenon seen at the macroscale and MD simulations can give us a better understanding of how to solve the challenges of prediction, efficiency, and convenience.

The purpose of this study is to understand bubble dynamics at the nano-scale and to evaluate the effect of temperature on the dispersion and the release of oxygen molecules from water. A clearer understanding of dissolving oxygen at the nanoscale can help predict oxygen concentration under various conditions and may be able to help design more efficient DAF systems. The visualization of the oxygen molecules and water droplet interaction at the nanoscale will also give understanding of the phenomenon of oxygen being released from water.

2. Method

This study was conducted using molecular dynamics simulations to model oxygen molecules being released by a water droplet at the nanoscale. A parallel MD program called NAMD(Phillips et al., 2005) was used to simulate the movement of molecules by adding up the forces on each atom and solving Newton's equation of motion for a time step of 2.0 fs. The forces are calculated using bonded and non-bonded potentials. The bonded potentials are the atomic bonds and angles between the atoms. The van der Waals and electrostatic potentials are the non-bonded potentials. The van der Waals potential is calculated using the Lennard Jones equation

$$U_{LJ} = 4\varepsilon_{ij}\left[\left(\frac{R_{\min}}{r_{ij}}\right)^{12} - \left(\frac{R_{\min}}{r_{ij}}\right)^{6}\right] \quad (1)$$

where r_{ij} is the distance between atoms i and j, and ε_{ij} is the characteristic energy and R_{min} is the van der Walls radius. The van der Waals potential quickly decays as the distance between the atoms increase so a sufficient cutoff radius of 12 Å was used to reduce computational time along with a smoothing function

between 10 Å and 12 Å. The velocity Verlet algorithm was used in addition to the Ewald method which calculated long-range electrostatic interactions. Simu -lations were run in the canonical ensemble also known as NVT ensemble meaning N (the number of atoms in the system), V (the system's volume), and T (the absolute temperature) were held constant using the velocity scaling method.

Simulations of 31002 TIP3P water molecules were run along with 100 oxygen molecules. The TIP3P (Transferable Intermolecular Potential, 3 Point) water model is a water model which combines realistic molecule interactions without using excessive computation time. The TIP3P water molecule has three charges, +0.417 e for the H atoms and -0.834 e for the O atom. The equilibrium angle between the atoms was set to 104.52 and uses Lennard-Jones parameters of R_{min} = 3.15061 Å and ε = 0.152 kcal/mol. As interactions between different substances occurred the characteristic energy used was $\varepsilon_{ij} = (\varepsilon_i \varepsilon_j)^{1/2}$. For the oxygen molecules the Lennard-Jones parameter of R_{min} = 2.99 Å was used corresponding to that found in the study of Zambrano et al.(2014).

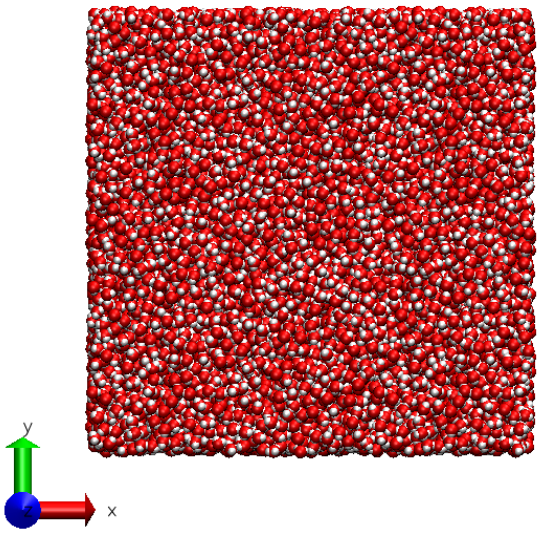

Fig. 1. The initial water cube with 100 Å sides.

Periodic boundary conditions were imposed to simulate an infinite domain. Simulations were run for an initial water box of 31002 water molecules at a constant temperature for 10 ns. An initial water cube with 100 Å sides as in Fig. 1 was centered at the origin. In the middle of the initial water cube water molecules were removed from a cube of 30 Å sides centered at the origin and 100 oxygen molecules were inserted in that vacant space. The computational domain was set to a cube with 150 Å sides centered at the origin.

Simulations were run at 0℃, 20℃, 40℃, 60℃, 80℃, and 100℃. The initial water cube quickly formed a sphere and oxygen molecules gradually began to escape the water droplet. At every nanosecond oxygen molecules which grouped together forming a quasi nano-bubble were counted along with the oxygen molecules that escaped the droplet.

3. Results and discussion

As simulation began, the initial hollow water box with oxygen molecule aligned inside began to change. The box morphed into a spherical water droplet and the oxygen molecules started to slowly move toward the periphery. Within 0.5 ns the water droplet had achieved a spherical shape for all cases considered. In Fig. 2 the dispersion of the oxygen molecules can be seen for a simulation run at 20℃. In the snapshots the water molecules are red and white points and the oxygen molecules are green and enlarged to be able to clearly see their positions. Fig. 2(a) is a snapshot of the molecules after 0.05 ns of simulation. The water still generally has a box shape that will soon change into a spherical droplet. The oxygen molecules are still bunched in the middle of the water droplet and are beginning to move toward the outside. Fig. 2(b) is a snapshot of the simulation at 2.0 ns. The water has clearly formed a spherical droplet due to the attractive forces and the oxygen

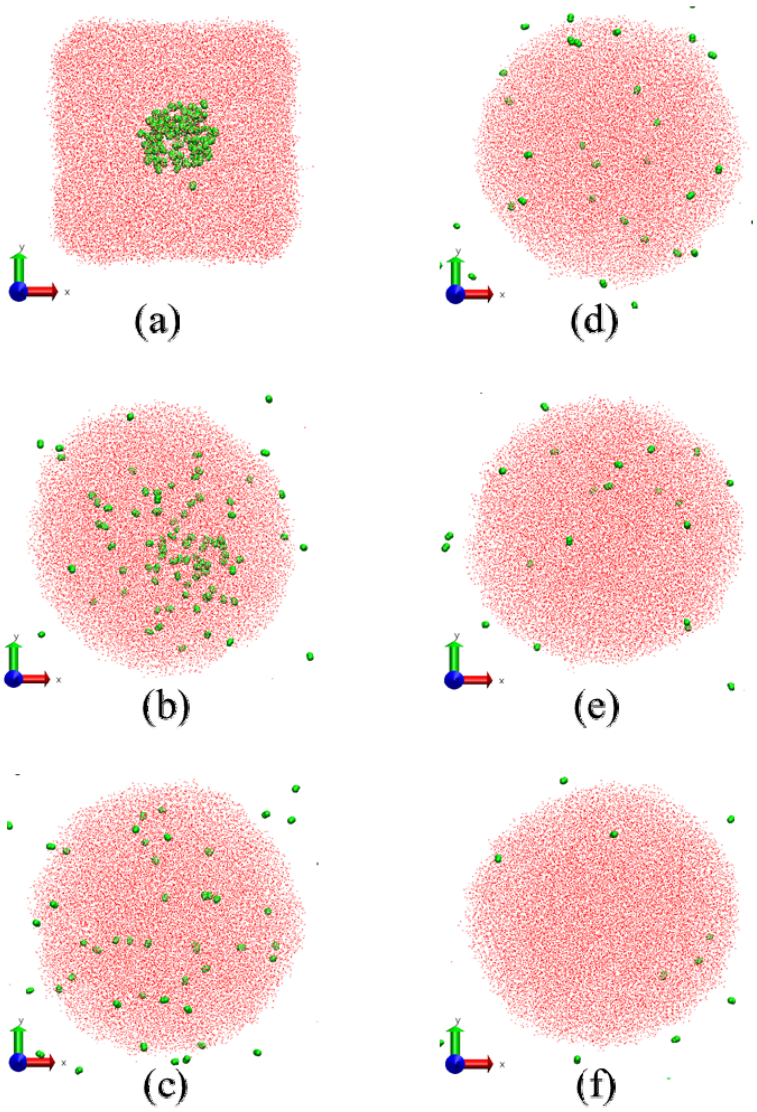

Fig. 2. Visualizations of oxygen being released from the water droplet at 20℃ after simulations times of (a) 0.05 ns (b) 2.0 ns (c) 4.0 ns (d) 6.0 ns (e) 8.0 ns (f) 10.0 ns.

molecules have spread throughout the droplet. Some molecules can be seen outside of the water droplet. The kinetic energy oxygen molecules cause the oxygen molecules to escape the attractive forces of the water molecules. Figs. 2(c), 2(d), 2(e), and 2(f) are snapshots of the simulation at 4.0 ns, 6.0 ns, 8.0 ns, and 10.0 ns, respectively. As time goes on, more and more oxygen molecules escape the water droplet until all of the oxygen molecules have escaped. This phenomenon occurred in all simulations.

The oxygen molecules freely moved around in the water droplet until it reached the edge of the water droplet where it either moved back toward the inside of the water droplet or hesitated before being released

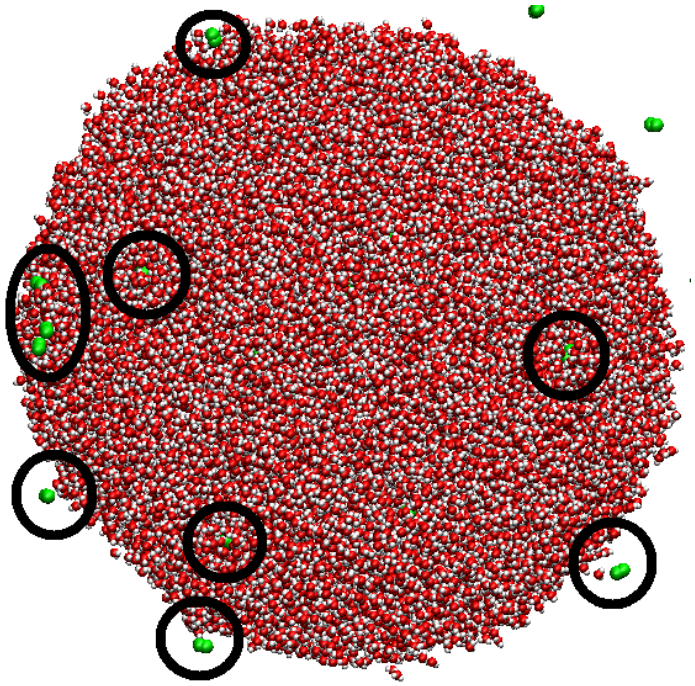

Fig. 3. Oxygen molecules near the edge of the water droplet. Some of these molecules immediately escaped the water droplet. Others did not.

from the water droplet. Inside the droplet the attractive forces of the water molecules were somewhat evenly distributed around the oxygen molecules, so the movement of the oxygen molecules was rather random and did not move in one direction. However at the edge of the water droplet, all of the surrounding molecules were pulling the oxygen molecules toward the water droplet. The kinetic energy of the oxygen molecules had to overcome the attractive forces of the surrounding water molecules to escape from the water droplet. It is difficult to see in the 2-dimensional figures but as the oxygen molecules seemed to hesitate at the edge of the water droplet there was a higher concentration of oxygen molecules near the edge of the droplet than the interior of the droplet after 4 ns of the simulation. A high concentration of oxygen molecules at the edge of the water droplet can be seen in Fig. 3. Furthermore, once an oxygen molecule escaped the water droplet it could move faster than before not being inhibited by the attractive forces of the water molecules. However, in a few cases, the oxygen molecules moved back in the vicinity of the water droplet and if the kinetic energy of the oxygen molecules was not strong enough and away from the water droplet, it was pulled back to the surface of the water droplet and sometimes engulfed by the water molecules again. Some of the water molecules also escaped the water droplet but the number of those molecules was insignificant compared to the whole, however as the temperature increases more and more water molecules were seen escaping the water droplet as expected.

After each nanosecond the oxygen molecules were categorized into three groups. Group 1 included oxygen molecules surrounded by other oxygen molecules in

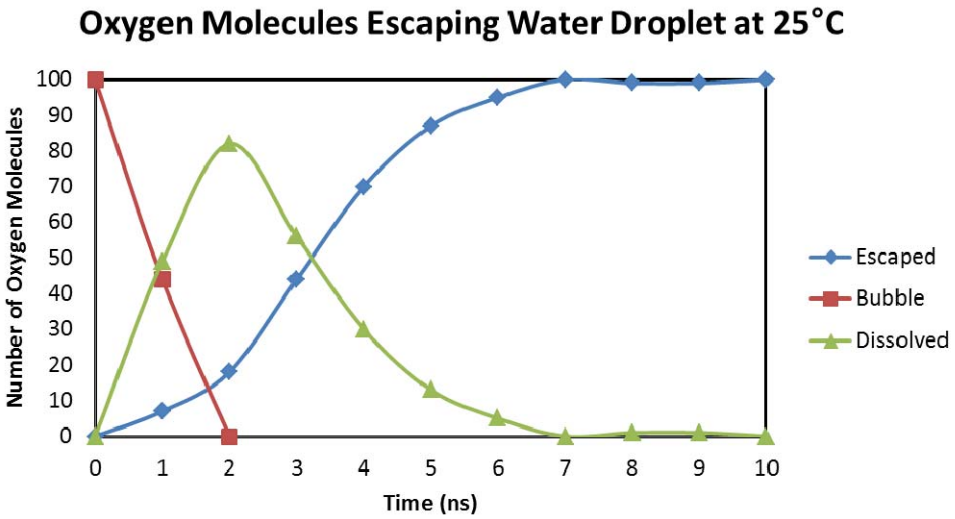

Fig. 4. Oxygen molecules in the bubble, dissolved, and escaped phase for 10 ns of simulation at 25℃.

the center of the water droplet which was called a bubble. Group 2 included oxygen molecules surrounded by water molecules. These oxygen molecules were considered dissolved. Group 3 included the oxygen molecules that had been released from the water droplet. Fig. 4 shows the number of the oxygen molecules in each group as the simulation progressed for the MD simulation at 25℃. At the beginning of the simulation all of the oxygen molecules composed a bubble at the center of the water droplet. As the simulation progressed, the oxygen molecules spread throughout the water droplet and the number of oxygen molecules in bubble decreased. By 2.0 ns none of the oxygen molecules remained grouped as a bubble. At that time, the number of oxygen molecules dissolved in the water droplet was at a peak of 82 molecules. The remaining 18 molecules had already escaped the water droplet.

The molecules quickly transitioned from the bubble phase to the dissolved phase, however transitioning from the dissolved phase to the escaped phase was slower and more gradual due to the attractive forces holding the oxygen molecules to water droplet as described before. Before 4 ns of simulation more oxygen molecules have escaped than have not. Between 2 ns and 4 ns the rate of molecules escaping was high and linear at 26 molecules / ns. At that point, the rate of release reduced until all oxygen molecules had escaped at 7ns. However, at 8 ns we found that one of the released oxygen molecules had re-entered the water droplet and remained there until just before the simulation had finished at 10 ns.

To further investigate the phenomenon of oxygen molecules escaping a nano-sized water droplet, simulations were carried out for different temperatures. Initially temperatures of 10℃, 20℃, and 25℃ were simulated but it was difficult to analyze the effect of temperature with such small temperature differences. Additional simulations were run between 0℃ and 100℃ with 20℃ intervals. These results can be seen in Fig. 5. As expected, the simulations with higher temperatures show oxygen molecules leaving the water droplet sooner and at a faster rate.

For the 100℃ case, 58 molecules escaped in the second nanosecond of simulation. This was clearly the highest rate of release among all of the cases

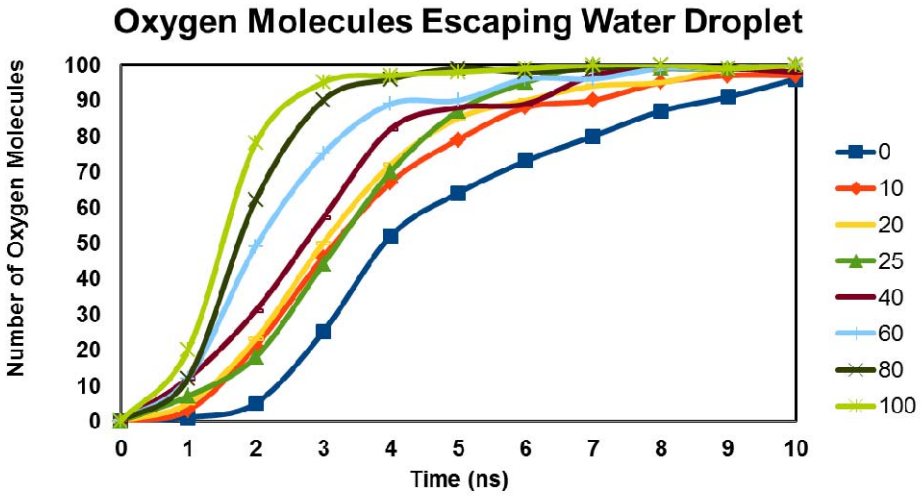

Fig. 5. Dissolved oxygen molecules in the nano-sized water droplet at different temperatures.

considered. The higher temperature gives the oxygen higher kinetic energy and causes the oxygen molecules to escape the droplet quickly. During the third nanosecond of simulation the escape rate significantly decreased as fewer oxygen molecules were available to escape the droplet. Then from 3 ns to 7 ns the rate of release of the remaining 5 oxygen molecules was nearly constant until all of the oxygen molecules had escaped before 7ns. At ns 9, one oxygen molecule had re-entered the water droplet before leaving by the end of the simulation.

In general all of the simulations followed this process. After the oxygen molecules leave the bubble phase the highest rate of release occurs. This was followed by a decrease in the escape rate until all of the oxygen molecules had escaped or the simulation ended. It can be seen that at higher temperatures that the escape rate was highest earlier in the simulation namely in the second nanosecond. The highest rate of release for 100℃ is in the second nanosecond which was 58 molecules / ns while the highest rate of release for 0℃ is in the fourth nanosecond of simulation. That rate of release was 27 molecules / ns. As the temperature decreases, the peak rate of release decreases for each respective temperature and occurs later in the simulation.

After the peak rate of release occurs, the rate of release decreases more dramatically at higher temperatures. After the peak rate of release for 100℃ in the second nanosecond the rate of release decreases 70.7% to 17 molecules / ns in the following nanosecond. For the 0℃ case, after the peak in the fourth nanosecond the rate of release decreases 55.6% to 12 molecules / ns in the fifth nanosecond. At that point the rate of release for the 0℃ case is nearly constant until the end of the simulation at an average of 6.4 molecules / ns. During that same period during the last 5 ns of the simulation the 100℃ case had an average escape rate of 0.4 molecules / ns due to the fact that 98% of all of the molecules had already escaped before the fifth nanosecond. This demonstrates that at higher temperatures there is a more pronounced move toward equilibrium than at lower temperatures where slower more gradual transitions are seen.

It can also be seen that after about 80% of the

molecules have escaped there are small fluctuations in the rate of release of the oxygen molecules for all temperatures. This phenomenon can easily be seen with the 40℃ simulation in Fig. 6. In the fifth nanosecond 6 oxygen molecules escaped while in the sixth and seventh nanoseconds 1 molecule and 8 molecules escaped respectively. This phenomenon is due to the large number of oxygen molecules in the domain that have already escaped. A number of those molecules are re-entering the water droplet giving the appearance that only a few molecules are escaping the water droplet in the sixth nanosecond of the 40℃ simulation, for example.

4. Conclusion

In this study 100 oxygen molecules were surrounded by 31002 water molecules and molecular dynamics simulations were carried out at different temperatures ranging from 0℃ to 100℃. With MD simulations molecules were visualized to help understand the interactions at the nano-scale. It was seen that the oxygen molecules could move inside of the nano-sized water droplet. However, once the oxygen molecules reached the edge of the water droplet, the oxygen molecules seemed to hesitate before escaping the water droplet. This occurred due to the attractive forces of the water molecules on the oxygen molecules. Once an oxygen molecule escaped the reach of the attractive forces of the water molecules, it could move freely in the rest of the domain without being inhibited by the water molecules. It was also recorded that the oxygen molecules transitioned from the bubble phase to the dissolved phase faster than the oxygen molecules transitioned from the dissolved phase to the escaped phase. This was attributed to the hesitation of the oxygen molecules at the edge of the water droplet. Also, the simulations with higher temperatures show oxygen molecules leaving the water droplet sooner and at a faster rate. As the temperature increases, there is a decrease in the highest rate of release for each temperature also increases and that peak rate of release occurs earlier in the simulation. At higher temperatures there is a quicker transition toward equilibrium than at lower temperatures. Furthermore, it can also be seen that after about 80% of the molecules have escaped there are small fluctuations in the rate of release of the oxygen molecules due to some oxygen molecules re-entering the water droplet. Through this investigation the rate of oxygen dispersion and phenomenon at the water's edge could be visualized giving a deeper understand of water-oxygen interaction at the nano-scale.

Acknowledgement

This study was made possible thanks to the 2014 research funding from the Catholic University of Pusan.

REFERENCES

Agarwal, A., Ng, W. J., Liu, Y., 2011, Principle and applications of microbubble and nanobubble technology for water treatment, Chemosphere, 84(9), 1175-1180.

Ambrosia, M. S., Ha, M. Y., Balachandar, S., 2013, The effect of pillar surface fraction and pillar height on contact angles using molecular dynamics, Applied Surface Science, 282(1), 211-216.

Bahadori, A., Zahedi, G., Zendehboudi, S., Bahadori, M., 2013, Estimation of air concentration in dissolved air flotation (DAF) systems using a simple predictive tool, Chemical Engineering Research and Design, 91(1), 184-190.

Dickinson, E., Ettelaie, R., Murray, B. S., Du, Z., 2002, Kinetics of disproportionation of air bubbles beneath a planar air–water interface stabilized by food proteins, Journal of Colloid and Interface Science, 252(1), 202-213.

Hami, M. L., Al-Hashimi, M. A., Al-Doori, M. M., 2007, Effect of activated carbon on BOD and COD removal in a dissolved air flotation unit treating refinery wastewater, Desalination, 216(1-3), 116-122.

Nagayama, G., Tsuruta, T., Cheng, P., 2006, Molecular dynamics simulation on bubble formation in a nanochannel, International Journal of Heat and Mass Transfer, 49(23-24), 4437-4443.

Papadopoulou, V., Tang, M., Balestra, C., Eckersley, R. J., Karapantsios, T. D., 2014, Circulatory bubble dynamics: From physical to biological aspects, Advances in Colloid and Interface Science, 206(4), 239-249.

Phillips, J. C., Braun, R., Wang, W., Gumbart, J., Tajkhorshid, E., Villa, E., Chipot, C., Skeel, R. D., Kalé, L., Schulten, K., 2005, Scalable molecular dynamics with NAMD, J. Comput. Chem., 26, 1781-1802.

Sulman, H. L., Picard, H. F. K., Ballot, J., 1905, Ore concentration, US Patent, No. 835120.

Thompson, P. A., Troian, S. M., 1997, A general boundary condition for liquid flow at solid surfaces, Nature, 389(6649), 360-362.

Zambrano, H. A., Walther, J. H., Jaffe, R. L., 2014, Molecular dynamics simulations of water on a hydrophilic silica surface at high air pressures, Journal of Molecular Liquids, 198, 107-113.

Zhang, Q., Liu, S., Yang, C., Chen, F., Lu, S., Bioreactor consisting of pressurized aeration and dissolved air flotation for domestic wastewater treatment, Separation and Purification Technology, 138, 186-190.

Zimmerman, W. B., Tesař, V., Bandulasena, H. C. H., 2011, Towards energy efficient nanobubble generation with fluidic oscillation, Current Opinion in Colloid & Interface Science, 16(4), 350-356.